Analytical Approach to Characterize Tornado-Induced Loads on Lattice Structures

Alice Alipour, M.ASCE[1]; Partha Sarkar, F.ASCE[2]; Saransh Dikshit[3]; Alireza Razavi[4]; and Mohammad Jafari[5]

Abstract: This paper presents a quasi-steady technique that combines aerodynamic force coefficients from straight-line wind tunnel tests with empirically developed tornado wind speed profiles to estimate the time history of aerodynamic loads on lattice structures. The methodology is specifically useful for large and geometrically complex structures that could not be modeled with reasonable scales in the limited number of tornado simulation facilities across the world. For this purpose, the experimentally developed tornado wind speed profiles were extracted from a laboratory tornado wind field and aerodynamic force coefficients of different segments of a lattice tower structure were assessed for various wind directions in a wind tunnel. The proposed method was then used to calculate the wind forces in the time domain on the model lattice tower for different orientation angles with respect to the tornado's mean path based on the empirical tornado wind speed profiles and the measured aerodynamic force coefficient of each tower segment, where the wind field at the tower location was updated at each time step as the tornado went past the tower. A tornado laboratory simulation test was conducted to measure the wind loads on a scaled model of a lattice tower subject to a translating tornado for the purpose of validation of the proposed method. The moving average of the horizontal wind force on the lattice tower model that was calculated with this method compared very well with that measured in a laboratory tornado simulator, which paves the way for the use of straight-line wind tunnels to assess tornado-induced loads on a lattice structure and possibly other similar structures. **DOI:** 10.1061/(ASCE)ST.1943-541X.0002660. *© 2020 American Society of Civil Engineers.*

Introduction

Many transmission towers, TV towers and antennas, communication towers, and open-roof trusses are made up of lattice structures. These structures are vital to the everyday life of communities and their failure can result in major socioeconomic impact. As such, it is important to assess their vulnerability to high-intensity winds (HIWs) such as hurricanes, tornadoes, and microbursts. Localized severe wind events in the form of downbursts and tornadoes are shown to be the source of 80% of weather-related failures in transmission towers alone ([ASCE 2010](); [Dempsey and White 1996]()). These meteorological phenomena are localized and unpredictable, rendering the capability to measure their scale, intensity, and structure using conventional recording stations in the field. The design of lattice structures based on straight-line wind events, where the velocity profile for a boundary-layer wind is used, which assumes a log law or power law along the height, accounts for the variation of mean wind velocity with height. The wind fields associated with

HIWs have different wind profiles and unique characteristics compared to those for boundary-layer wind fields. The localized nature of HIWs and the shape of the gust changes the line of action of the wind loads, normally moving it closer to ground level. Furthermore, specific to tornadoes, the wind profile has a significant rotational and vertical component of velocity with accelerations. The velocity fields are three dimensional and structural loading effects are transient in nature.

The effects of tornadoes on lattice structures can generally be divided into two major steps: (1) characterizing the tornado wind speed profiles using tornado simulation through experiments or computational fluid dynamics (CFD), and (2) understanding structural performance of lattice structures under tornado loads generated with simulated wind fields of tornadoes. For instance, Wen ([1975]()), Wen and Ang ([1975]()), and Savory et al. ([2001]()) attempted to simplify the model for a tornado by utilizing a three-dimensional flow in the boundary layer of the tornado-like vortex where the tangential, radial, and vertical wind velocity profiles are functions of radial distance and height. Mehta et al. ([1976]()) developed analytical models of a tornado and calculated the loads on buildings from poststorm damage investigations. The maximum wind speed in the tornadic wind was determined from calculation of equivalent straight-line wind capable of producing the same building failure. A major disadvantage of this method is that the tornado loads were considered to be steady state, which led to inaccurate load values that underestimated the number of failures during tornadoes.

Specific to transmission towers, El Damatty et al. ([2014]()) discussed advancement in tornado wind field measurements in addition to various numerical methods to simulate these events. It was concluded that the size and location of the tornado relative to the lattice transmission tower structure are important to the magnitude of wind loads on the lattice tower. Hamada et al. ([2010]()) established a numerical approach to assess the performance of transmission lines under tornado wind loads. The tornado wind field was based on a model-scale CFD analysis that was conducted and validated in

[1]Assistant Professor, Dept. of Civil, Construction and Environmental Engineering, Iowa State Univ., Ames, IA 50011. ORCID: https://orcid.org/0000-0001-6893-9602. Email: alipour@iastate.edu

[2]Professor, Dept. of Aerospace Engineering, Iowa State Univ., Ames, IA 50011 (corresponding author). Email: ppsarkar@iastate.edu

[3]Ph.D. Student, Dept. of Civil, Construction and Environmental Engineering, Iowa State Univ., Ames, IA 50011. ORCID: https://orcid.org/0000-0002-4872-0635

[4]Senior Instructor, School of Engineering, Dunwoody College of Technology 818 Dunwoody Blvd, 55403 Minneapolis, Minnesota, USA.

[5]Ph.D. Candidate, Dept. of Aerospace Engineering, Iowa State Univ., Ames, IA 50011.

a previous study. Later, Hamada and El Damatty (2015) provided a detailed approach to modeling the critical tornado wind speed profiles for transmission towers. Most recently, El Damatty and Hamada (2016) developed the wind speed profiles for transmission lines using a series of experimental tests in tornado simulators that are introduced in the ASCE Manual No. 74 (2010) design guidelines. Hamada (2014) numerically modeled two lattice transmission towers and carried out a parametric study to identify the critical tornado locations leading to peak forces on the structure, followed by failure analysis under these critical cases. El Damatty et al. (2018) carried out a study for the finite-element models of the transmission line systems by considering the tornado wind fields from a 2005 Kansas tornado. Teoh et al. (2019) used a dynamic wind simulation on a series of power poles to study the damage to the structures and evaluate the life-cycle cost considering aging and wind effects.

It is observed that the available studies on characterization of loads either rely on highly expensive experimental simulations or computationally time-consuming CFD models or utilize simplified assumptions in coming up with the empirical models for tornado wind speed profiles. The developed performance models are specific to the structure that is exposed to either experimental or CFD-based tornado wind fields. Thus, there is a lack of a general approach for simulating the effects of a translating tornado on lattice structures that provides a quick and less costly but accurate representation of the variable nature of the wind loads on these structures. This is particularly necessary because available tornado simulators are limited in number, with only three available in North America: Iowa State University (Haan et al. 2008) and Texas Tech University (Tang et al. 2018) in the US and Western University in Canada (Refan and Hangan 2016). The available tornado simulators are relatively small in size and cannot accommodate models of lattice structures such as those in TV antennas and transmission towers with adequate scaling because of the blockage effects ratio of the projected area of the model in plan or elevation with respect to the respective area of the tornado core. Furthermore, they are incapable of accurately reproducing and measuring the effects of turbulence arising from wind flow over the open or suburban terrain where most tower structures are located because of their relatively small fetch. On the other hand, despite some recent advancements, which are limited to predicting wind loads on simple buildings in nonsynoptic wind events, numerical methods (such as CFD) fall short in replicating many aspects of the complex flow field and their interaction with structures.

This paper proposes an alternative approach for calculating the wind loads on lattice structures owing to a tornado. The paper aims to extend the capability of subsonic wind tunnel facilities to replicate the effects of HIWs on lattice structures. For this purpose, the features of a 500-kV transmission tower is used to present the proposed procedure. The procedure includes (1) use of tornado wind speed profiles including their empirical forms based on measurements in a laboratory tornado simulator (P. P. Sarkar, "Empirical tornado and downburst wind speed profiles," working paper), (2) estimation of the aerodynamic force coefficients of different segments of the lattice tower based on their section models in a uniform wind flow generated in a wind tunnel, and (3) estimation of the total wind loads experienced by the tower under different simulated tornado scenarios and validating them using data from the laboratory tornado simulator. The merit of this study exists in eliminating the need to carry out computationally intensive numerical simulations or expensive experimental tests for estimating the wind loads on a lattice tower during a tornado. The approach is shown to be able to assess the mean shear forces, and should the turbulence be modeled in the wind field and admittance functions of the structure estimated, it can be even used to assess the

dynamic buffeting loads. The proposed method uses a quasi-steady approach to predict the mean wind loads on a lattice tower in a translating tornado by using empirical-laboratory-derived wind speed profiles of a tornado and combining them with mean two-dimensional aerodynamic force coefficients for different segments of the lattice tower as measured in wind tunnels that are widely available to the community. This relatively simple method to estimate wind loads on a lattice tower in a tornado enhances the capability of the natural hazards engineering community to characterize the HIW-induced loads on lattice structures; this approach can be easily extended to other types of nonsynoptic wind events such as downburst and gust fronts.

Laboratory-Based Tornado Load Simulation

This section discusses the capabilities of the Iowa State University tornado simulator (ISU-TS), the details associated with the experimental setup, and the data collected from the conducted tornado simulations on a model transmission tower.

Tornado Simulator

The laboratory tornado simulation has become an acceptable method for estimating tornado wind loads on civil structures. ISU-TS has contributed to this effort over more than a decade. This section briefly describes the tornado vortex generation mechanism of this facility. A 1.83-m-diameter fan at its center sucks air upward, simulating an updraft that passes through a series of screens and a honeycomb that tries to eliminate effects of the fan on the upstream flow, before turning into a horizontal duct composed of two spaced circular plates, then flowing radially outward at the top of the simulator. The flow gains angular momentum after passing through a series of equally spaced vanes and hinged flat plates placed along the outer periphery of the circular plates at a fixed angle. The rotating flow is then guided downward through a vertical duct at the outer section of the simulator, where it resembles the downdraft occurring in tornadoes. The downdraft flows onto the ground plane and inward toward the tornado center before it reaches the updraft region to complete the circuit. To simulate translating tornadoes, the simulator is suspended above the ground plane by a 5-t crane and can be moved on a straight line with a maximum speed of 0.61 m/s. The schematic illustration and more details about the simulator are available in Haan et al. (2008).

The controlling parameters of ISU-TS were set to simulate a tornado with medium swirl ratio after vortex touchdown and before evolution of multiple vortices. Critical nondimensional parameters (Lewellen 2012; Church et al. 1979) like swirl ratio, radial Reynolds number, and aspect ratio were calculated using Eqs. (1)–(4). These parameters define the structure of the stationary tornado that was used to simulate the translating one

$$S_c = \frac{r_c \Gamma}{2Q'h} = \frac{r_c \cdot 2\pi r_c V_{\theta c}}{2Q} = \frac{\pi r_c^2 V_{\theta c}}{Q} = 0.25 \quad (1)$$

$$S_{\text{vane}} = \frac{\tan \theta}{2a} = 0.86 \quad (2)$$

$$a = \frac{h}{r_o} = 0.84 \quad (3)$$

$$Re_r = \frac{Q'}{2\pi\nu} = 1.68 \times 10^5 \quad (4)$$

where $V_{\theta c}$ = maximum mean tangential velocity in the flow field (10.8 m/s) that occurs at an elevation z_c (0.05 m); r_c = core radius

(0.32 m) at which $V_{\theta c}$ occurs; S_c = swirl ratio at r_c, Γ = circulation defined at r_c; Q' = volume flow rate per unit inlet height; h = inlet height (0.76 m); Q = volume flow rate (12.03 m³/s); S_{vane} = swirl ratio at the radial location of the vanes; θ = vane angle relative to the radial direction (55°); a = aspect ratio; r_o = fan radius (0.91 m); Re_r = radial Reynolds number; and ν = kinematic viscosity of air (1.5×10^{-5} m²/s). Variable S_c is an alternate definition of swirl ratio, initially given by Haan et al. (2008) to relate swirl ratio to characteristic velocity and length, $V_{\theta c}$ and r_c, in the tornado wind field. The simulated tornado had a translational velocity of 0.5 m/s. The velocity scale was estimated by comparing the maximum horizontal velocity of the laboratory tornado, 12.1 m/s, with the maximum horizontal velocity of a design tornado for which a highly important structure such as a transmission tower should be designed. Because a majority of tornadoes in the US are of EF3 or smaller intensity, the maximum mean hourly equivalent wind speed of an EF3 tornado (73 m/s 3-s gust or 47.7 m/s mean hourly) can be used to estimate the velocity scale $\lambda_v = 12.1/47.7 = 1/3.9$. Thus, a translation speed of 0.5 m/s of the laboratory tornado scales up to 1.95 m/s (4.4 mi/h) in full scale, which is a translation speed of a slowly moving tornado in the field similar to the Manchester, South Dakota, tornado of 2003 (2.2 m/s) (Karstens et al. 2010).

Experimental Setup

A scaled model ($\lambda_L = 1:120$) representing a 500-kV transmission tower (variant-148M single-circuit type) was tested in ISU-TS. Selection of this length scale results in area ratio of 0.05 between projected plan area of the structure and area of the tornado core region. This ratio guarantees that peak wind pressure and wind force coefficients are independent of the size of the structure. The full model and its dimensions are shown in Fig. 1. To measure the wind loads on the transmission tower model in ISU-TS, an aluminum rod was attached to the model that passed through its center and fixed to its top. The model was fixed on the ground plane of ISU-TS to a 3-axis load sensor (JR3, Woodland, CA) placed underneath it by this rod that passed through an orifice in the ground plane. The load sensor was capable of measuring forces and moments in all the three directions. It has a precision of $\pm 0.25\%$ of its full range of 40 N (along the vertical or Z-axis) and 30 N (along the X- or Y-axis or its in-plane). The sampling rate for the data was set at 1,000 Hz.

A schematic view of the scaled model placed in the tornado simulator setup with its coordinate system and lateral positioning are shown in Fig. 2. The tower was located at two lateral locations along the Y-direction (Fig. 3) to represent the distance of the tower from the mean tornado path that is along the X-axis. This distance is normalized by the core radius (r_c). The mean tornado path is defined as the midlocation of the region where the maximum pressure drop occurs for all the load cases used here. The tests were carried out for three tower orientation angles (α) of 0°, 45°, and 90°. Orientation angle is defined as the angle between the principal axis of the transmission tower (X_m) and translation direction of the tornado (X) as in Fig. 3. Along with different tower orientation angles, the horizontal distance from the center of the mean tornado path to the center of the transmission tower was varied as 0 and 30.5 cm (12 in.) to simulate cases where the tornado passes the center of the tower or follows a localized path away from the tower. The tornado translated with a speed of 0.5 m/s for all of the considered scenarios. The test cases and the corresponding illustrations are shown in Fig. 3. For each case, 10 data runs were taken and the average of the parameters was extracted from the data, i.e., forces along the X- and Y-directions, to provide better statistics.
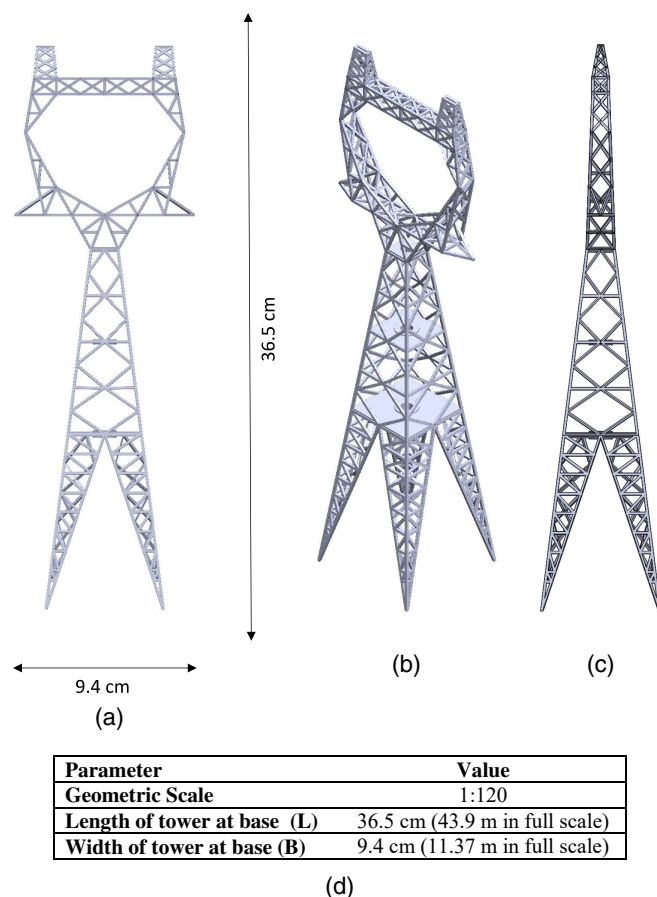

Fig. 1. Scaled model of transmission tower for experimental tests: (a) isometric view; (b) view in the longitudinal direction (X_m-direction); (c) view in the transverse direction (Y_m-direction); and (d) tabulated model and full-scale dimensions.

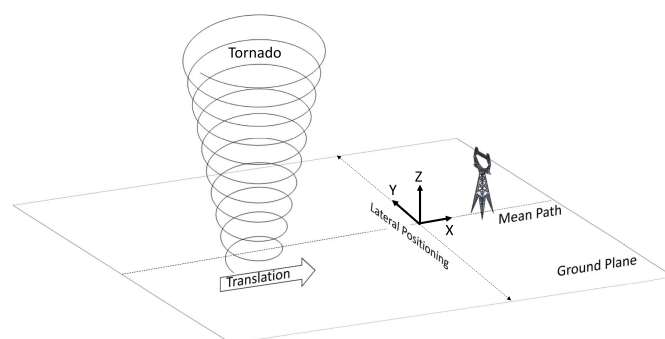| Parameter	Value
Geometric Scale	1:120
Length of tower at base (L)	36.5 cm (43.9 m in full scale)
Width of tower at base (B)	9.4 cm (11.37 m in full scale)

(d)

Fig. 2. Coordinate system and lateral positioning of the transmission tower under Case 1.

Based on a study by Kikitsu and Okuda (2016), the relative size of the building model to the tornado size above a critical value affects the measurements of surface pressures and loads on a test model in tornado simulators, which is like a blockage effect of models in regular wind tunnels. To determine the adequacy of the model size with respect to measurement error of tornado-induced loads in the laboratory, Kikitsu and Okuda defined a model size to tornado size ratio to determine the relative size of the model
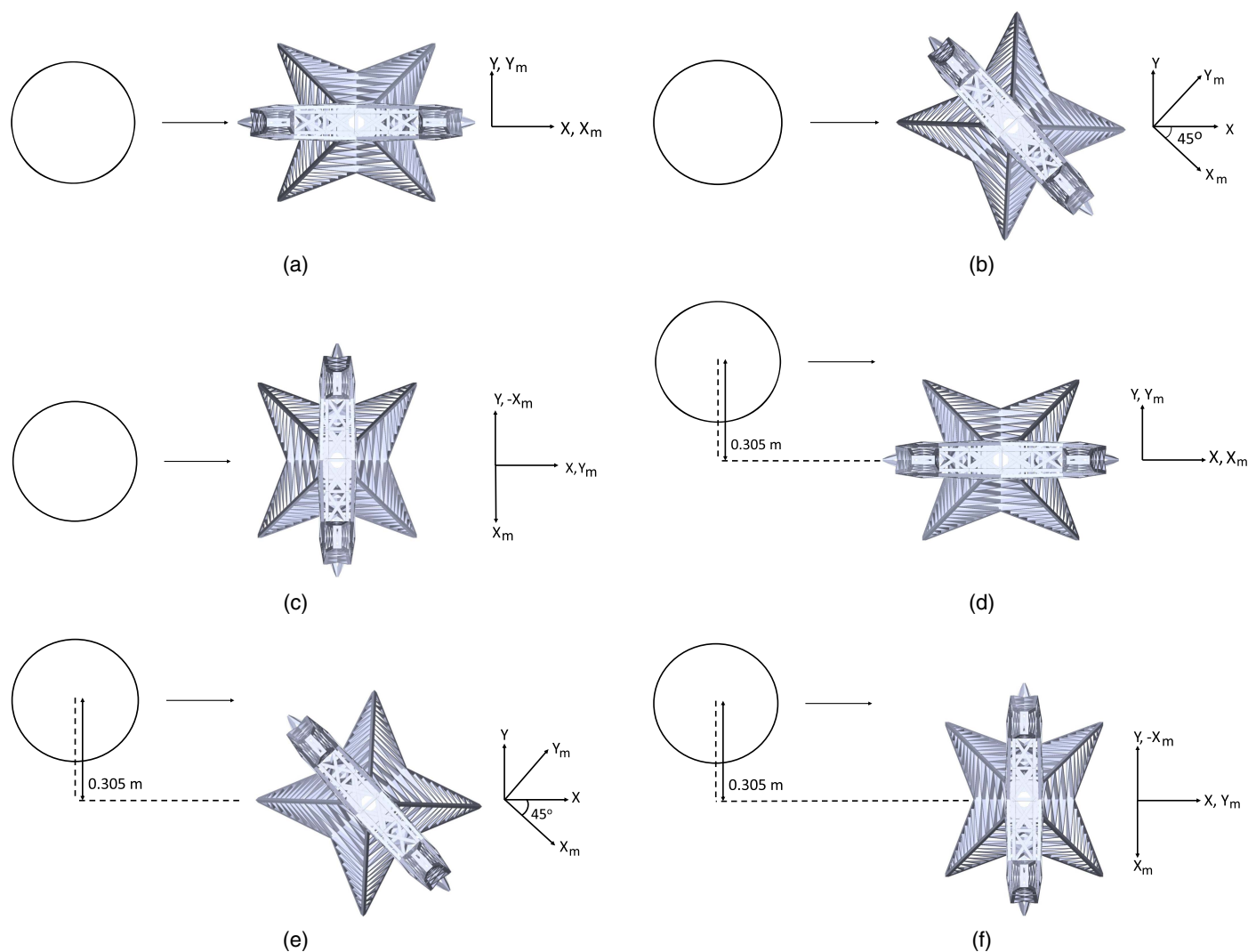
© ASCE

04020108-3

J. Struct. Eng.

Fig. 3. Different cases for simulation and tower orientation: (a) Case 1; (b) Case 2; (c) Case 3; (d) Case 4; (e) Case 5; and (f) Case 6.

to the tornado core as the ratio of the radius of the equivalent circular area of the model plan area to the radius of the core of simulated tornado [Eq. (5)]

$$r_r = \frac{r_{eq}}{r_c} = \frac{1}{r_c}\sqrt{\frac{BL}{\pi}} \tag{5}$$

where r_r = model size to tornado size ratio, which is the relative size of a model to the core of simulated tornado; r_c = radius of the core; and r_{eq} = radius of the equivalent circular area of the tower plan area (BL), where B and L are maximum width and maximum length of the model, respectively.

Kikitsu and Okuda suggested that the model size to tornado size ratio be limited to 0.45 or even lower, if possible. A lower model size to tornado size ratio leads to a reduced blockage effect of the model immersed inside the laboratory tornado and ensures more accurate measurement of tornado-induced loads by not adversely affecting the tornado flow structure by the model. The model size to tornado size ratio in the current tests is equal to $0.105/0.32 = 0.33$ (model plan area is $0.365 \times 0.094 = 0.034$ m^2, $r_{eq} = 0.105$ m), which is much lower than the critical value of 0.45.

Load Time Histories

Typical velocity components associated with a translating tornado are shown in Fig. 4. The figure shows a tornado with a translating velocity V_T, which has two components of velocity on the horizontal plane: the radial component V_r and the tangential component V_θ. The tornado center is located at distance r from the transmission tower. Owing to these two velocity components, the tower experiences velocity in the radial and tangential directions that constantly changes in magnitude and direction as the distance r changes. These tower velocity components, V_r (r, z) and V_θ (r, z), vary with
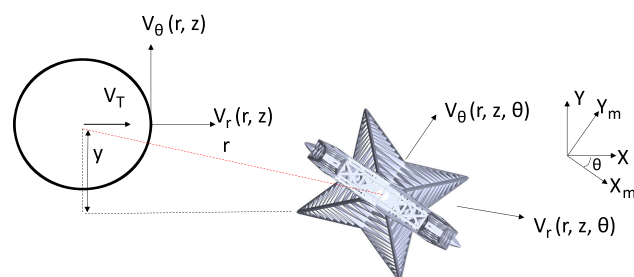

Fig. 4. Velocity components associated with a translating tornado.

elevation and hence along the height of the transmission tower. There is also a vertical component, $V_z(r, z)$, of the velocity in a tornado, the effect of which is neglected on the horizontal loads on the tower, which is an open-framed structure.

The experimental results obtained from the ISU tornado simulator tests for all the load cases identified in Fig. 3 are shown in

Fig. 5. In Fig. 5, C_{Fx} and C_{Fy} are normalized components of the horizontal shear force along the absolute coordinate system that does not change with orientation of the tower. The difference in the X and Y forces and reversal pattern is a result of the combination of wind speed magnitude, direction and force coefficients, projected areas, tower orientation, location, and pressure drop profile.
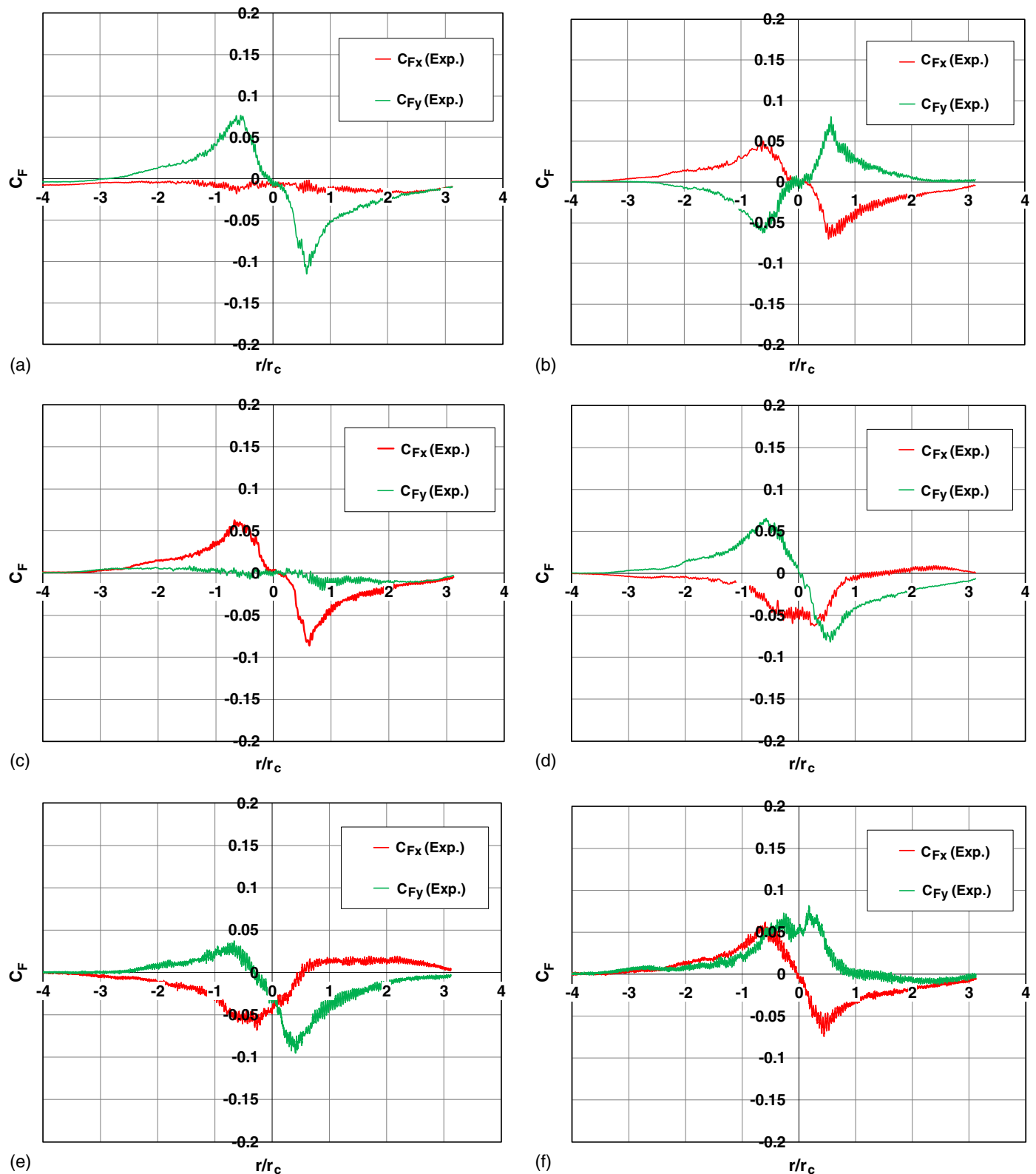

Fig. 5. Experimental load time histories for (a) Case 1; (b) Case 2; (c) Case 3; (d) Case 4; (e) Case 5; and (f) Case 6.

Analytical Tornado Load Estimation

This section provides an overview of the current approaches to estimate tornado loads on towers, develops a series of empirical tornado profiles that are generated based on the experimental tornado simulations, discusses the proposed analytical methodology for estimation of loads on lattice structures, and presents a comparison on the results from experimental and proposed analytical methods.

State-of-the Art Approach in Calculating Tornado Loads

The current approach to design transmission towers is to follow ASCE Manual No. 74 (2010) for design of latticed steel transmission structures. This manual provides a method of calculating the forces owing to a tornado by considering the gust response factor, G, velocity pressure coefficient, K_z, and a load factor of 1.0, respectively. Wind loading corresponding to a moderate tornado (F1 or F2) is applied to the full structure height by considering the maximum horizontal wind speed for the given scale. In general, the velocity and turbulence intensity profiles are quite different from a regular atmospheric boundary layer (ABL) straight-line wind for which structures are designed. While there have been attempts to include more reasonable tornado profiles in the manual (El Damatty and Hamada 2016), there are still no clear guidelines as to how the tornado loads will be estimated from the tornado wind velocity profiles.

Most design codes (IEC 2003; CSA 2004) use a global approach to estimate the loads on lattice towers. This method is based on the solidity ratio of the lattice structure, which represents the ratio of the projected area to the total area, which is a measure of the obstruction and flow momentum loss caused by the lattice structure. Fundamental sources in wind engineering (Blevins 2003) and a few design codes (e.g., IEC 2003) provide equations that relate the solidity ratio to the tower orientation angle that are adopted from earlier tests (e.g., Georgiou and Vickery 1979; Lindley and Willis 1974; Whitbread 1979). However, because of the irregular shape of these towers, using one solidity ratio for the whole tower introduces a great deal of uncertainty. The method ends up using the same drag coefficient for the truss of a certain solidity ratio regardless of the different wind directions it experiences. Furthermore, the drag coefficient for two truss segments that look different but with the same solidity ratio is taken to be the same.

A review of the literature shows that the aerodynamic coefficients for different configurations of transmission towers are rarely available (Deng et al. 2016). A few researchers have attempted to develop local approaches where the wind forces are evaluated in straight-line conditions on each truss member separately and then summed to assess the total wind forces exerted on the structure (Prud'homme et al. 2014, 2018). The method, although promising, is shown to be infeasible in cases of a transmission tower where there are hundreds of truss members with different orientations and alignments. For this purpose, this paper proposes the use of wind load coefficients generated from straight-line wind tunnel tests to assess the tornado-induced wind forces on different segments of the tower by combining them with the wind speeds and wind directions estimated from empirical-experimental tornado wind speed profiles to assess the exerted wind loads experienced by the structure. It is believed that such approach would provide better estimates of the aerodynamic drag forces on the tower caused by the translating tornado.

Empirical Tornado Velocity Profiles

Because of the nonstationarity of the flow, it is common to perform repeated testing on the scaled models of structures in tornado simulators to obtain tornado loads on the structure. This is an expensive and time-consuming approach. Additionally, access to such facilities is limited. To address this issue, profiles of the radial and tangential wind speeds of the tornado could be derived based on laboratory data to estimate the wind loads acting on the transmission tower. The empirical wind profiles of the tangential wind speed of a stationary tornado with a two-celled structure used here were proposed by P. P. Sarkar on the basis of multiple data sets obtained from ISU-TS as published by Sarkar and his co-workers for the simulated tornado (Sarkar 2019).

The tangential wind speed profiles for a tornado with a core radius of r_c are classified into three categories: (1) within the core ($0.5r_c \leq r < r_c$), (2) vicinity of core boundary ($r = r_c$), and (3) outside the core ($r > 1.2r_c$). Constants associated with these profiles are derived for a translating tornado. The equations of the tangential wind speed profiles are as follows:

$$V_\theta(r, z) = V_{\theta\max}(z)\left(\frac{r}{r_c}\right)^\alpha \quad 0 \leq r \leq r_c \quad (6)$$

$$V_\theta(r, z) = V_{\theta\max}(z) \quad r_c \leq r \leq 1.2r_c \quad (7)$$

$$V_\theta(r, z) = V_{\theta\max}(z)\left(\frac{1.2r_c}{r}\right)^\eta \quad r \geq 1.2r_c \quad (8)$$

where $\alpha = 1.25$ (for a two-celled tornado with medium swirl like the ones used for this study); $V_{\theta\max}(z) =$ maximum tangential wind speed of the tornado at a given height (z); and $\eta = 1.2$ (degradation rate).

The variation of the tangential wind speed with respect to the height (z) can be calculated by the following equations:

$$\frac{V_{\theta\max}(z)}{V_{\theta\max}(z_c)} = C_1\left(\frac{z}{z_c}\right)^\beta \left[1 - \text{erf}\left(C_2\frac{z}{z_c}\right)\right] \quad z \leq 3.5z_c \quad (9)$$

$$\frac{V_{\theta\max}(z)}{V_{\theta\max}(z_c)} = C_1\left(\frac{z}{z_c}\right)^\gamma \quad 3.5z_c \leq z \leq 12z_c \quad (10)$$

where $C_1 = 1.1$; $C_2 = 0.08$; $\beta = 0.10$; $\gamma = -0.018$; $z =$ elevation from ground; and $z_c =$ height at which absolute maximum largest value of the tangential wind speed $V_{\theta\max}$ occurs in the flow field. Fig. 6 shows the experimental radial wind speed profiles that were used for interpolation and Fig. 7 shows the derived empirical
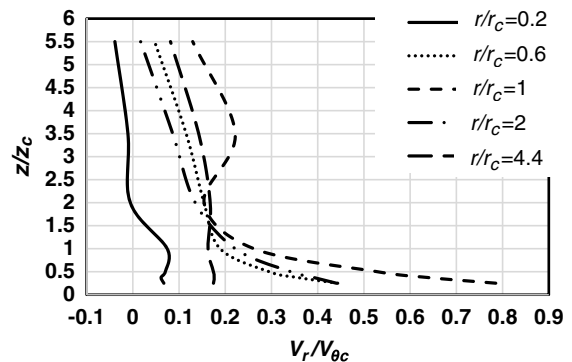

Fig. 6. Experimental radial profiles used for interpolation. (Data from Razavi and Sarkar 2018a, b, c.)
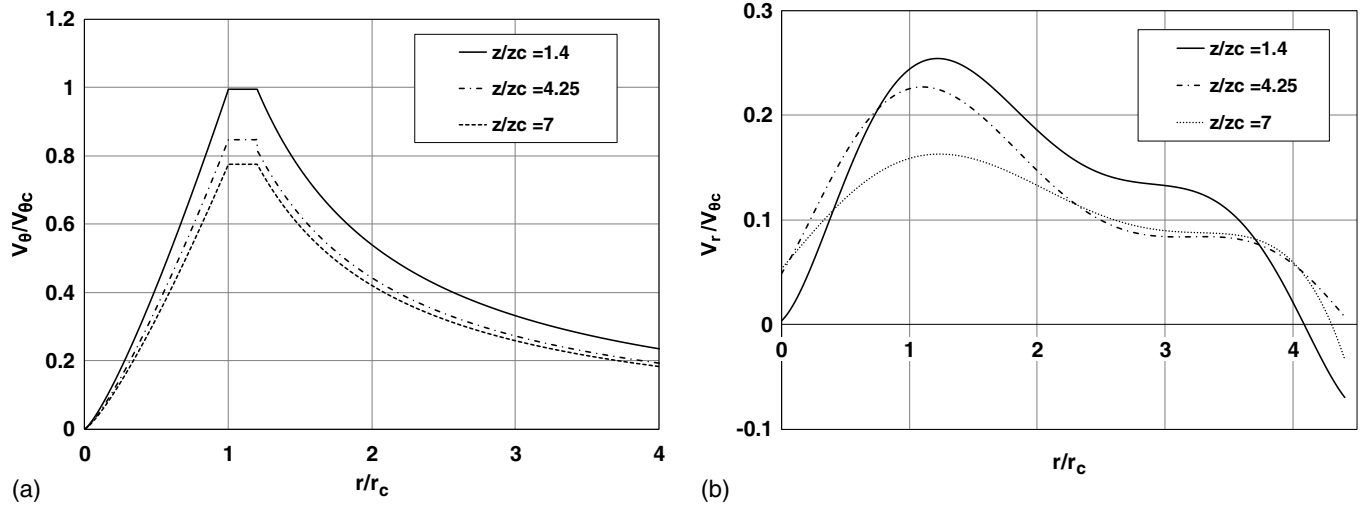
© ASCE

04020108-6

J. Struct. Eng.

Fig. 7. (a) Empirical tangential wind speed profiles (data from Sarkar 2019), and (b) radial wind speed profiles (data from Razavi and Sarkar 2018a, b, c) for a stationary tornado.

tangential wind speed profiles and the interpolated radial profiles of the wind speed at three elevations (z/z_c = 1.4, 4.25, 7.0) that are midheights of the three tower sections used in this study. The positive values of radial velocities shown in Fig. 7 are in the opposite direction to r, positive toward the center of tornado.

Fig. 7 shows the empirical form of the tangential wind speed profile for a stationary tornado. Deriving a universal form of the radial wind speed profile was not an easy task because it changes continuously and drastically with distances r and z. Thus, the radial wind speeds in this study at a given location (r, z) were obtained by interpolation from the radial wind speed profiles measured at discrete locations of a stationary tornado in ISU-TS by Razavi and Sarkar (2018a, b, c).

The resultant horizontal wind speed, V_H, can be calculated using the following equation:

$$V_H = \sqrt{V_{xm}^2 + V_{ym}^2} \tag{11}$$

where V_{xm} and V_{ym} = components of wind speed along the principal axes of the tower at a given elevation (z) that are functions of tangential wind speed V_θ (r, z, θ) and radial wind speed V_r (r, z, θ) of the stationary tornado at the radial location (r), orientation (θ), and elevation (z) of the tower. The angle V_H makes with respect to the model axis X_m can be calculated using the ratio of V_θ (r, z, θ) and V_r (r, z, θ) and tower orientation angle. The vector summation of the translation velocity of the tornado V_T (= 0.5 m/s here) and V_H provides the resultant velocity V_{Tor} of the approaching tornado at the location of the transmission tower at a given elevation. Based on the wind speed for the tornado (V_{Tor}) and with the known dimensions of the scaled model, the shear forces acting on the scaled model can be calculated if accurate estimates of the force coefficients exist. The estimation of shear force coefficient for the tower and how it varies with the translating tornado are discussed in the following section.

Estimates of Shear Force of a Transmission Tower in a Tornado

Comparing the tornado wind speed profiles along the height of the tower (Fig. 8), one can observe that in addition to the tower shape variability along the height (and hence projected area), the wind

speed profile is also variable. This highlights that using only one set of aerodynamic coefficients for the tower could result in notable erroneous results. To address this issue the tower was divided into three segments (Fig. 9) that represent the legs, the midsection, and the top section of the tower, and the aerodynamic coefficients were generated for each segment. In Fig. 9, A_S and A_T are the solid areas and total areas for each of the sections.

At this stage, drag and lift coefficients for the three segments of the tower were measured in the aerodynamic test section of the Aerodynamic-Atmospheric Boundary Layer (AABL) Wind and Gust Tunnel located at Iowa State University under uniform and smooth (<0.2% turbulence intensity) flow on section models of the tower segments. This wind tunnel is primarily a closed-circuit
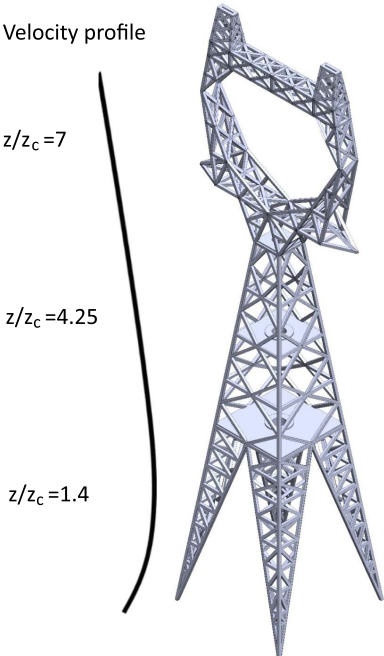

Fig. 8. Variation in tornado velocity profile with height of tower and the highly variable tower geometry along the height.
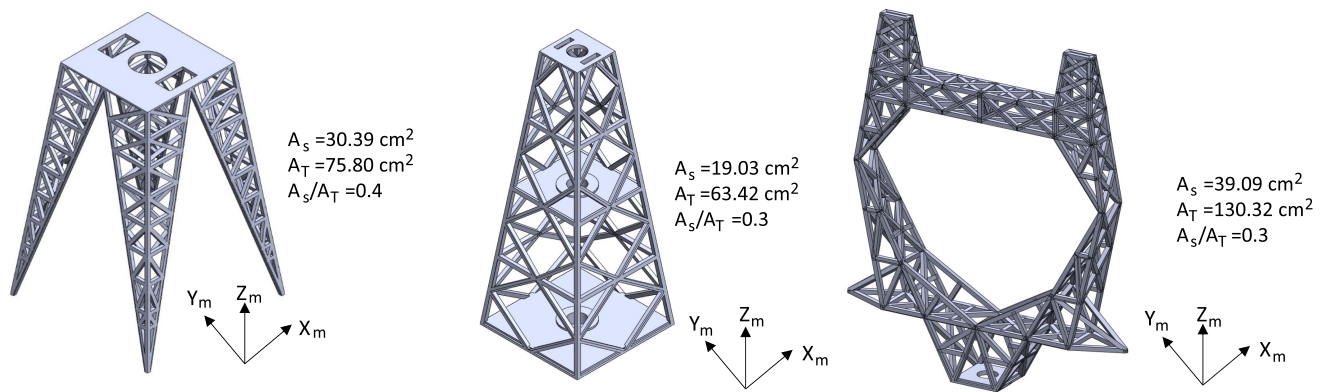
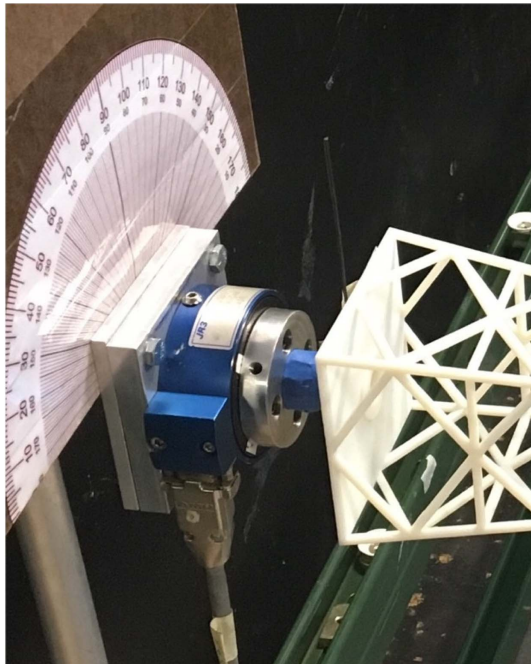**Fig. 9.** Three segments of the transmission tower model.

Fig. 10. Tower section model attached to JR3 load sensor in the wind tunnel.

Fig. 11. Experimental setup showing the three section models of the transmission tower tested in the ISU AABL wind and gust tunnel (side view).

Fig. 12. Tower model with definition of tower orientation angle (α).

tunnel with two test sections (aerodynamic: 2.44×1.83 m and ABL: 2.44×2.21 m) with maximum wind speeds up to 53 m/s. Figs. 10 and 11 show the test setup for the static tests for each of the three tower segments.

Fig. 10 shows a typical model of a tower segment fixed to a JR3 load sensor with a protractor behind it to help in adjusting the wind angle of attack of the model. The geometric or length scale of each of three models shown in Fig. 11 is 1:110. End plates were not used in these models because these are not two-dimensional sections, unlike typical section models that have uniform cross section along their length. The end plates on a typical section model in a normal flow are used to ensure two-dimensional flow around the model, but the flow around the tower section models used here was three dimensional because these models are nonuniform along its length. There is a socket in the JR3 sensor that was meant for attaching the tower section model. A small cylindrical tube was fixed at the base of the section model to attach it to the JR3 sensor by inserting it into the sensor socket. When calculating the drag force on the tower
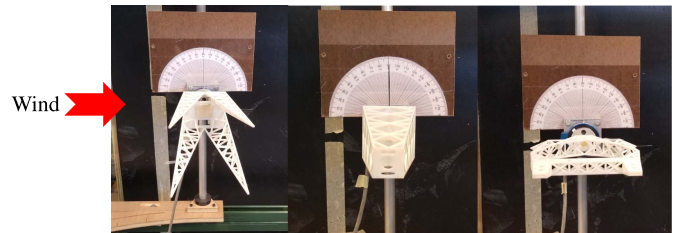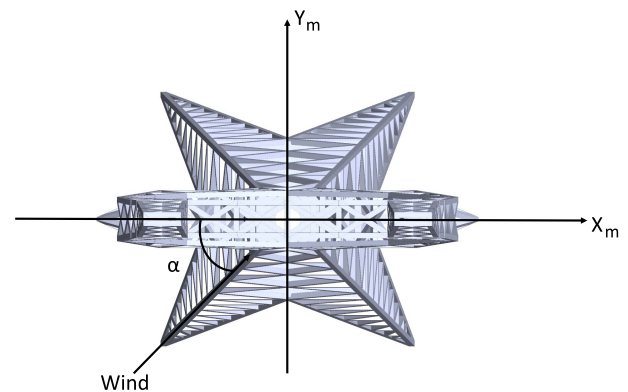
section model, the drag force on the cylindrical tube was subtracted to get the actual drag force on the tower section model.

The loads on the lattice tower segments were measured using a six-component load sensor (JR3) that included the three components of forces and moments in the X-, Y-, and Z-directions. Fig. 12 shows the top view of the transmission tower model and the tower orientation angle (α) that is defined with respect to the principal axis X_m of the tower model. For force measurements, the sampling rate and sampling time were 500 Hz and 60 s, respectively. The section model of each section of the transmission tower was rotated along the model axis that is perpendicular to the wind flow to obtain the different angles of attack. The angles were measured by a protractor attached to the probe.

The calculated blockage ratio was less than 3% for all experiments. Tests were repeated for different orientation angles varying from 0° to 90° in increments of 10°. For each tower orientation angle, as defined in Fig. 12, the tests were conducted for a range of wind speeds (9.89, 13.78, 17.68, 20.27 m/s). It is a standard practice to use multiple wind speeds (four in this study) to ensure consistency between the measurements at different wind speeds for the Reynolds numbers used here. The drag and lift coefficients measured in this study for the four considered wind speeds were found to be independent of Reynolds number in the range of wind speed used in this study. These velocities can be compared with the maximum mean hourly equivalent wind speed of an EF3 tornado (73 m/s 3-s gust or 47.7 m/s mean hourly) to estimate the velocity scale varying from 1:4.8 to 1:2.4. Time and frequency scales can be calculated from length and velocity scales as $\lambda_t = 1/46$ (min) and $\lambda_f = 46/1$, respectively, for these tests. Thus, 60 s of data as measured in the wind tunnel would scale up to 46 min of full-scale data, which was considered adequate to estimate the mean aerodynamic loads. The average of the drag and lift coefficients for the different wind speeds for a given tower orientation angle were taken for that particular tower orientation angle.

Once the drag and lift coefficients were obtained, they were resolved along the model coordinate system to get the force coefficients C_{Fxmi}, C_{Fymi} in the X_m and Y_m directions as functions of the tower orientation angle (α). Eqs. (12) and (13) show the formulation for obtaining the force coefficient in the X_m and Y_m directions, respectively

$$C_{Fxmi} = C_{Di} \cos \alpha - C_{Li} \sin \alpha \qquad (12)$$

$$C_{Fymi} = C_{Di} \sin \alpha + C_{Li} \cos \alpha \qquad (13)$$

where C_{Di} and C_{Li} = drag and lift coefficients obtained for each of the test sections, respectively.

Fig. 13 shows the force coefficients for each of the sections in the X_m and Y_m directions obtained using Eqs. (12) and (13). These coefficients were later used in calculating the aerodynamic forces in the X_m and Y_m directions for simulating the tornado loads. The components of the aerodynamic shear force (F_{xmi}, F_{ymi}) for each of the three segments of the tower ($i = 1$–3) were calculated using the horizontal wind speed V_{Tor} in a tornado experienced by these segments of the tower at its midheight and the components of the

aerodynamic force coefficients (C_{Fxi}, C_{Fyi}) for each corresponding segment, i, of the transmission tower. The total shear force (F_{xm}, F_{ym}) along each direction, X_m or Y_m, was obtained by summing the shear forces for each of the segments and comparing them with those of the corresponding loads measured in ISU-TS for verification. The two components of the aerodynamic shear force on the horizontal plane acting on the lattice tower can be calculated using Eq. (14)

$$F_{xm} = \sum 0.5 \rho V_{Tor,i}^2 C_{Fxi} L_{xi} D_{xi}, \quad F_{ym} = \sum 0.5 \rho V_{Tor,i}^2 C_{Fyi} L_{yi} D_{yi} \qquad (14)$$

where ρ = air density (= 1.23 kg/m³); $V_{Tor,i}$ = resultant horizontal wind speed at the midheight of the ith tower segment; C_{Fxmi} and C_{Fymi} = force coefficients of the corresponding ith segment of the tower along the X_m or Y_m direction; and L_{xi} and D_{xi}, L_{yi} and D_{yi} = projected area dimensions of the corresponding ith segment of the tower on a plane normal to the X_m or Y_m direction.

Analytical simulations were repeated for three tower orientation angles and two different locations of the tower with respect to the translating tornado and compared with the experimental results (Fig. 5). The components of the normalized shear forces F_{xm} and F_{ym} or shear force coefficients (C_{Fxm}, C_{Fym}) obtained in the X_m and Y_m directions, as normalized by a characteristic area A_C and maximum tangential wind speed $V_{\theta max}$, are defined in Eqs. (15)–(19)

$$A_X = H \times \text{maximum width of tower in } Y_m \text{ direction} \qquad (15)$$

$$A_Y = H \times \text{maximum width of tower in } X_m \text{ direction} \qquad (16)$$

$$A_C = \sqrt{A_X A_Y} \qquad (17)$$

$$C_{Fxm} = \frac{F_{xm}}{0.5 \rho V_{\theta max}^2 A_C} \qquad (18)$$

$$C_{Fym} = \frac{F_{ym}}{0.5 \rho V_{\theta max}^2 A_C} \qquad (19)$$

The analytical and experimental results of C_{Fxm} and C_{Fym} were compared for all the cases.

Fig. 14 shows that the analytical results present similar variations in the normalized shear force or shear force coefficient values and shapes as the experimental results. In Case 1 [Fig. 14(a)], the shear force in the X_m direction is significantly lower than the shear in the Y_m direction. This could be attributed to the tangential wind speeds the tower experiences that are aligned with the Y_m direction (transverse or minor axis of the tower). Case 2 in Fig. 14(b) shows the analytical and experimental shear forces when the tower orientation angle is 45°. Case 3 in Fig. 14(c) shows the opposite behavior of shear force components as the model is rotated by 90° compared to Case 1. This can be explained based on tangential wind speeds the tower experiences along the X_m direction (longitudinal or major axis of the tower). It can be seen that in Case 1 the peak on the right side (positive r/r_c) is higher than the peak on the left side (negative r/r_c). This could be because of the translation of the tornado that causes a decrease in the relative horizontal wind speed on the left side while causing an increase in the relative horizontal wind speed on the right side. For Case 2, where the model is oriented at an angle of 45° with respect to the tornado translation direction, the components of relative wind speed in the X_m and Y_m directions are similar, resulting in peak values that are similar in magnitude. Case 4 in Fig. 14(d) shows the result when the tower model and the tornado simulator are at a lateral offset value of 0.305 m and at
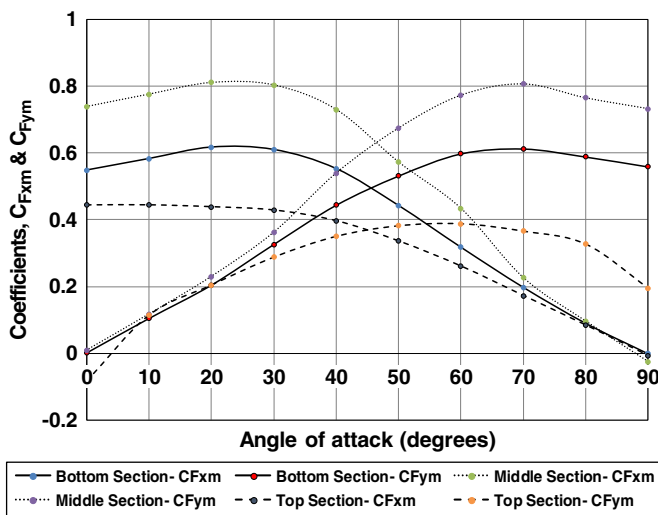

Fig. 13. Force coefficients (C_{Fxmi} and C_{Fymi}) for different tower segments as functions of tower orientation angle (or angle of attack, α).
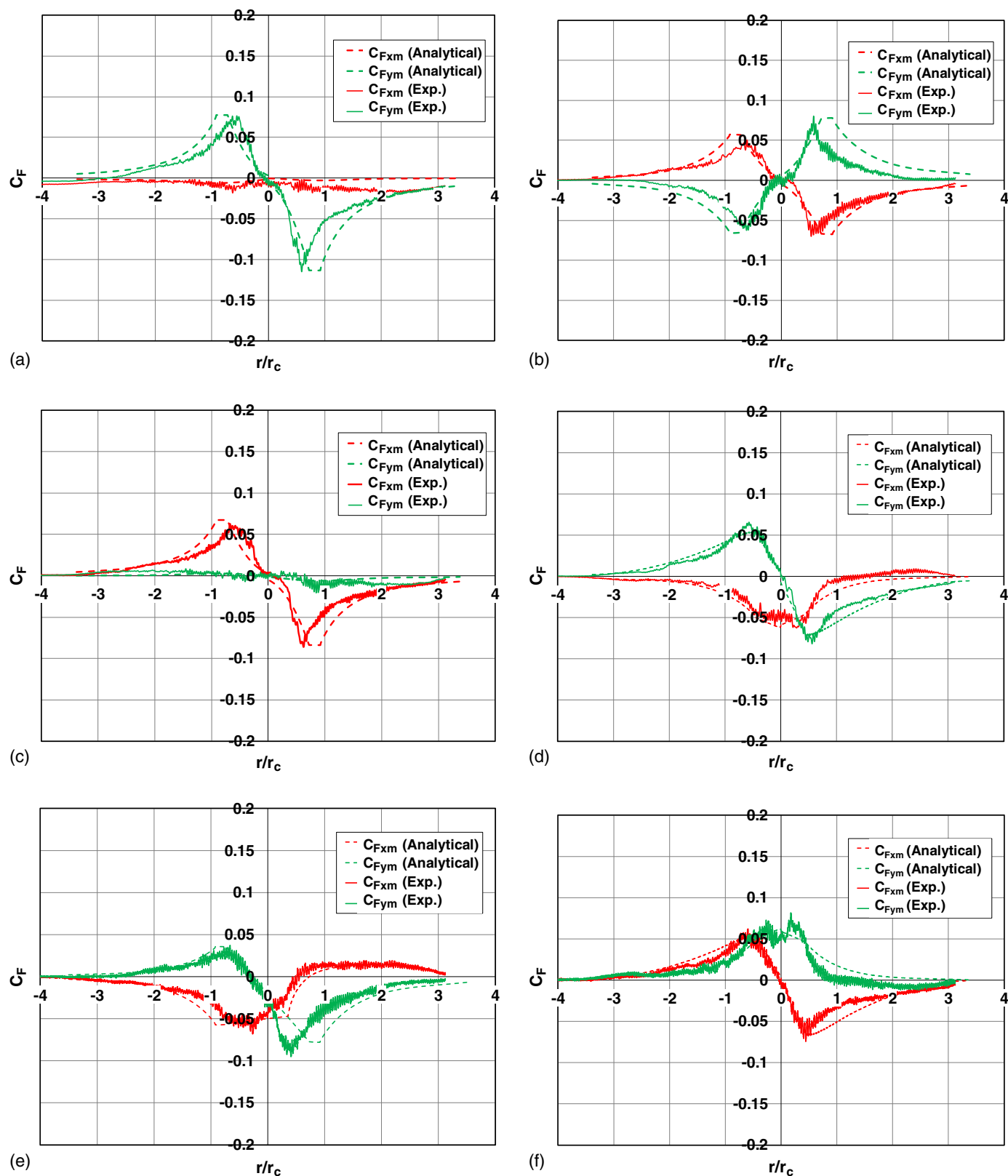
Fig. 14. Comparison of analytical and experimental results for (a) Case 1; (b) Case 2; (c) Case 3; (d) Case 4; (e) Case 5; and (f) Case 6.

tower orientation angle of 0°. The maximum shear force in the Y_m direction is similar but somewhat smaller than Case 1, while there is increase in the shear force in the X_m direction. This is primarily because the tangential wind speed direction is aligned with the X_m direction and maximum tangential wind speed occurs at around

this location of r_c (= 0.32 m). Cases 5 and 6 in Figs. 14(e and f) show the shear forces in the X_m and Y_m directions for the transmission tower when there is a lateral offset of 0.305 m with tower orientations of 45° and 90°, respectively. Results in Case 5 are similar to that of Case 4, but because the tower is oriented at an

angle of 45°, there is reversal of sign of the shear force in the X_m direction. Case 6 is the opposite of Case 4 in terms of shear forces. This is because of switching of the direction along which maximum wind speeds occur as seen by the tower in the X_m and Y_m directions.

The time lags between the two peak values (experimental versus analytical) for all the cases are because of transient effects that are intrinsically present in the aerodynamic loads generated in laboratory simulations of the translating tornado but not accounted for in the analytical simulations. Also, as the tornado translates in the
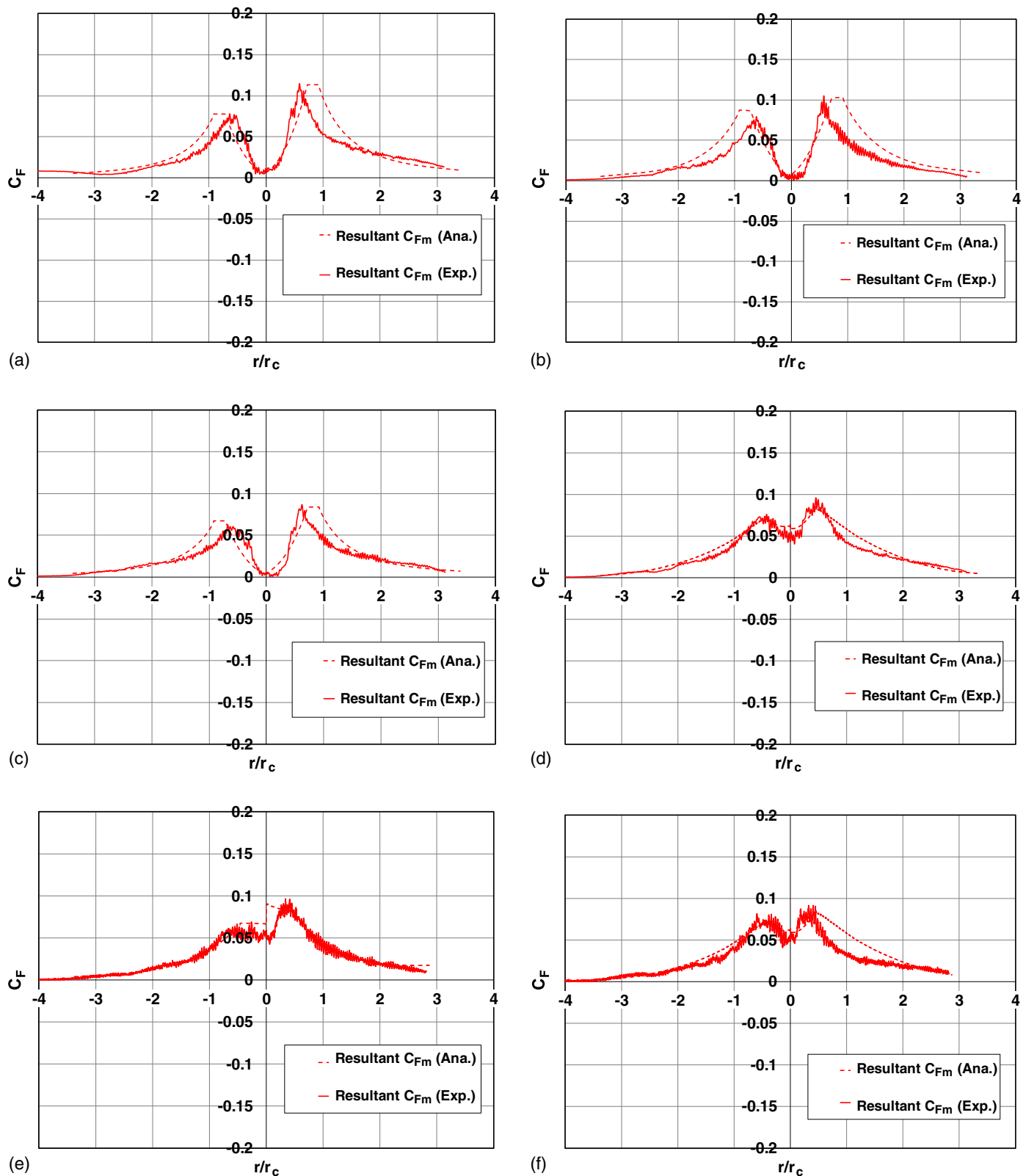
Fig. 15. Comparison of analytical and experimental results using total force that relates the drag coefficient at the specified direction to the instantaneous wind for (a) Case 1; (b) Case 2; (c) Case 3; (d) Case 4; (e) Case 5; and (f) Case 6.

laboratory simulation, the members of the tower model closest to the tornado center experience the effects of the tornado wind before the other members that are farther from it experience the same. The effects of static pressure drop around the tornado center that will have additional but minor effects on the shear force and vertical wind component that influences the vertical angle of attack and hence the aerodynamic loads are not accounted for in the proposed formulation. A third effect that introduces the lag time in the model loads is the fact that in laboratory tornado simulation the location of the tornado is measured based on the physical location of the tornado simulator, whereas the center of the tornado vortex at the ground has been observed to lag behind this location.

Because the proposed approach depends on the accuracy of the tornado wind speed model, an alternate approach that uses total force (i.e., $\sqrt{F_x^2 + F_y^2}$) is used that relates the drag coefficient at the specified direction to the instantaneous wind. Fig. 15 shows the results for the six cases considered where the resultant force net force vector is used and the results between the mean shear force and the tested time-varying mean force are compared.

Conclusions

This paper aims to develop an analytical approach for calculating the mean aerodynamic shear forces on a transmission tower subjected to tornado loading. The aerodynamic shear forces for six different cases were modeled using a conventional approach adopted by the current codes and a proposed approach. The proposed approach takes into account the effect of tower orientation angles and offset distance of the tower from the tornado mean path on the mean wind speeds and wind directions at the tower location. The analytical results were validated by experimental test results obtained from ISU-TS. Based on the results obtained, the proposed approach can provide a good representation of the actual loading on the transmission tower. In this method, the force coefficients of different tower segments were measured in a regular wind tunnel as a function of horizontal wind tower orientation angle or angle of attack, and were then incorporated into the analytical load estimation model. The results confirm the hypothesis that the capability of subsonic wind tunnel facilities could be used to replicate the effects of HIWs on large-scale structures. This relatively simple method to estimate the maximum mean wind load on a lattice tower in a tornado enhances the capability of the natural hazards engineering community to characterize HIW-induced loads on lattice structures; this approach can be easily extended to other types of nonsynoptic wind events such as downburst and gust fronts. This method can be extended further to capture the effects of turbulence, static pressure drop, and vertical wind speed on the wind loads.

Acknowledgments

References

ASCE. 2010. *Guidelines for electrical transmission line structural loading*. ASCE Manual No. 74, Reston, VA: ASCE.

Blevins, R. D. 2003. *Applied fluids dynamics handbook*, Malabar, FL: Krieger publishing.

Church, C. R., J. T. Snow, G. L. Baker, and E. M. Agee. 1979. "Characteristics of tornado-like vortices as a function of swirl ratio: A laboratory investigation." *J. Atmos. Sci.* 36 (9): 1755–1776. https://doi.org/10.1175/1520-0469(1979)036<1755:COTLVA>2.0.CO;2.

CSA (Canadian Standards Association). 2004. *Antennas, tower and antenna-supporting structures*. CSA S37. Rexdale, ON, Canada: CSA.

Dempsey, D., and H. B. White. 1996. "Winds wreak havoc on lines." *Transm. Distrib. World* 48 (6): 32–42.

Deng, H. Z., H. J. Xu, C. Y. Duan, X. H. Jin, and Z. H. Wang. 2016. "Experimental and numerical study on the responses of a transmission tower to skew incident winds." *J. Wind Eng. Ind. Aero.* 157 (Oct): 171–188. https://doi.org/10.1016/j.jweia.2016.05.010.

El Damatty, A., A. Elawady, A. Hamada, and W. E. Lin. 2014. "State-of-the-art knowledge about behaviour of transmission line structures under downbursts and tornadoes." In *Proc., World Congress on Advances in Civil, Environmental, and Materials Research*. Yuseong, Daejeon, Korea: IASEM and KAIST.

El Damatty, A., N. Esami, and A. Hamada. 2018. "Case study for behaviour of transmission line structures under full-scale flow field of Stockton, Kansas, 2005 tornado." In *Proc., Electrical Transmission and Substation Structures 2018*. Reston, VA: ASCE.

El Damatty, A., and A. Hamada. 2016. "F2 tornado velocity profiles critical for transmission line structures." *Eng. Struct.* 106 (Jan): 436–449. https://doi.org/10.1016/j.engstruct.2015.10.020.

Georgiou, P., and B. Vickery. 1979. "Wind loads on building frames." In *Proc., 5th Int. Conf. on Wind Engineering*, 421–433. Oxford: Pergamon Press.

Haan, F. L., Jr., P. P. Sarkar, and W. A. Gallus. 2008. "Design, construction and performance of a large tornado simulator for wind engineering applications." *Eng. Struct.* 30 (4): 1146–1159. https://doi.org/10.1016/j.engstruct.2007.07.010.

Hamada, A. 2014. "Numerical and experimental studies of transmission lines subjected to tornadoes." Ph.D. thesis. Dept. of Civil and Environmental Engineering, Univ. of Western Ontario.

Hamada, A., and A. El Damatty. 2015. "Failure analysis of guyed transmission lines during F2 tornado event." *Damatty Eng. Struct.* 85 (Feb): 11–25. https://doi.org/10.1016/j.engstruct.2014.11.045.

Hamada, A., A. A. El Damatty, H. Hangan, and A. Y. Shehata. 2010. "Finite element modelling of transmission line structures under tornado wind loading." *Wind Struct. Int. J.* 13 (5): 451–469. https://doi.org/10.12989/was.2010.13.5.451.

IEC (International Electrotechnical Commission). 2003. *Design criteria of overhead transmission lines*. IEC 60826. Geneva: IEC.

Karstens, C. D., T. M. Samaras, B. D. Lee, W. A. Gallus, and C. A. Finley. 2010. "Near-ground pressure and wind measurements in tornadoes." *Mon. Weather Rev.* 138 (7): 2570–2588. https://doi.org/10.1175/2010MWR3201.1.

Kikitsu, H., and Y. Okuda. 2016. "Tornado-induced wind load model on a building considering relative size of building and tornado-like vortex." In *Proc., 6th U.S.-Japan Workshop on Wind Engineering*, 12–14. Yokohama, Kanagawa: Yokohama National Univ. and Ames, IA: Iowa State Univ.

Lewellen, D. C. 2012. "Effects of topography on tornado dynamics: A simulation study." In *Proc., 26th Conf. on Severe Local Storms*, 5–8. Boston, MA: American Meteorological Society.

Lindley, D., and D. Willis. 1974. "Wind loads on transmission line towers."In *Proc., 5th Australian Conf. on Hydraulics and Fluid Mechanics*, 224–234. Christchurch, New Zealand: Univ. of Canterbury.

Mehta, K. C., J. R. McDonald, and J. Minor. 1976. "Tornadic loads on structures." In *Proc., 2nd USA–Japan Research Seminar on Wind Effects on Structures*, 15–25. Honolulu, Hawaii: Univ. of Hawaii.

Prud'homme, S., F. Legeron, A. Laneville, and M. K. Tran. 2014. "Wind forces on single and shielded angle members in lattice structures." *J. Wind Eng. Ind. Aero.* 124 (Jan): 20–28. https://doi.org/10.1016/j.jweia.2013.10.003.

Prud'homme, S., F. Legeron, and S. Langlois. 2018. "Calculation of wind forces on lattice structures made of round bars by a local approach."

Eng. Struct. 156 (Feb): 548–555. https://doi.org/10.1016/j.engstruct.2017.11.065.

Razavi, A., and P. P. Sarkar. 2018a. "Laboratory investigation of the effects of translation on the near-ground tornado flow field." *Wind Struct. Int. J.* 26 (3): 179–190. https://doi.org/10.12989/was.2018.26.3.179.

Razavi, A., and P. P. Sarkar. 2018b. "Laboratory study of topographic effects on the near-surface tornado flow field." *Boundary Layer Meteorol.* 168 (2): 189–212. https://doi.org/10.1007/s10546-018-0347-5.

Razavi, A., and P. P. Sarkar. 2018c. "Tornado-induced wind loads on a low-rise building: In fluence of swirl ratio, translation speed and building parameters." *Eng. Struct.* 167 (Jul): 1–12. https://doi.org/10.1016/j.engstruct.2018.03.020.

Refan, M., and H. Hangan. 2016. "Characterization of tornado-like flow fields in a new model scale wind testing chamber." *J. Wind Eng. Ind. Aero.* 151 (Apr): 107–121. https://doi.org/10.1016/j.jweia.2016.02.002.

Sarkar, P. P. 2019. *Empirical tornado and downburst wind speed profiles*, personal communication.

Savory, E., G. A. R. Parke, M. Zeinoddini, N. Toy, and P. Disney. 2001. "Modeling of tornado and microburst induced wind loading." *Eng. Struct.* 23 (4): 365–375. https://doi.org/10.1016/S0141-0296(00)00045-6.

Tang, Z., C. Feng, L. Wu, D. Zuo, and D. L. James. 2018. "Characteristics of tornado-like vortices simulated in a large-scale ward-type simulator." *Boundary Layer Meteorol.* 166 (2): 327–350. https://doi.org/10.1007/s10546-017-0305-7.

Teoh, Y. E., A. Alipour, and A. Cancelli. 2019. "Probabilistic performance assessment of power distribution infrastructure under wind events." *Eng. Struct.* 197 (Oct): 109–199. https://doi.org/10.1016/j.engstruct.2019.05.041.

Wen, Y. K., and A. H. S. Ang. 1975. "Tornado risk and wind effects on structures." In *Proc., 4th Int. Conf. on Wind Effects on Buildings and Structures*, 63–74. Cambridge, UK: Cambridge Univ..

Wen, Y.-K. 1975. "Dynamic tornadic wind loads on tall buildings." *J. Struct. Div.* 101 (1): 169–185.

Whitbread, R. E. 1979. "The influence of shielding on the wind forces experienced by arrays of lattice frames." In *Proc., 5th Int. Conf. on Wind Engineering*, 405–420. Oxford, UK: Pergamon press.